

COB-2023-1900
**EFFECT OF PRE-PLACED POWDERS OF GRAPHENE AND GRAPHITE
ON DILUTION AND HARDNESS OF STELLITE 6 COATINGS
PROCESSED BY PTA**

João Felipe Sippel

Graduation Program in Mechanical Engineering (PGMec), Federal University of Paraná (UFPR), Polytechnic Center, Av. Cel. Francisco H. dos Santos, 100 - Jardim das Américas, Curitiba - PR, Brazil, 81530-000
jfsippel@gmail.com

Willian Rafael de Oliveira

Instituto Engenharia de Superfícies, INCT/CNPq
Federal University of Paraná (UFPR), Polytechnic Center, Av. Cel. Francisco H. dos Santos, 100 - Jardim das Américas, Curitiba - PR, Brazil, 81530-000
wrofisica@gmail.com

Juliane Ribeiro da Cruz Alves

Graduation Program in Mechanical Engineering (PGMec), Federal University of Paraná (UFPR), Polytechnic Center, Av. Cel. Francisco H. dos Santos, 100 - Jardim das Américas, Curitiba - PR, Brazil, 81530-000
Senai Institute of Innovation in Laser Processing, R. Arno Waldemar Döhler, 308 - Santo Antônio, Joinville - SC, Brazil, 89218-153
juliane.rcruz@gmail.com

Ana Sofia C. M. d'Oliveira

Department of Mechanical Engineering, Federal University of Paraná (UFPR), Polytechnic Center, Av. Cel. Francisco H. dos Santos, 100 - Jardim das Américas, Curitiba - PR, Brazil, 81530-000
sofmat@ufpr.br

Abstract.

The tailoring of coatings by changing the chemical composition with graphite and graphene has demonstrated potential to improve mechanical and abrasive resistance by combining self-lubricating properties with superior strength. Among the alloys used for abrasive wear resistance applications Stellite 6 a CoCrWC-based alloy, is an industrial reference in applications where high resistance to wear, cavitation and high temperatures are required. Tailoring of coatings with additions of graphite and graphene have been carried out using techniques such as thermal spraying and thin films depositions. However, Stellite 6 hardfacing coatings modified by graphite and graphene have not yet been. This work is part of an on going project on tailoring Stellite 6 coatings processed by Plasma Transferred Arc for wear resistance applications. Particularly it addresses the addition of graphite and graphene to the Co-based alloy, as powder mixtures and as pre-placed powders. The pre-placed layers on the 304 stainless steel substrate was done on three different surface finishing: as cold-rolled, ground with #36 sandpaper and ground with # 220 sand paper. The objective is to investigate the influence of the surface roughness on anchoring and retention of these carbon-based particles, as well as its impact in bead characteristics and Vickers microhardness. Vickers microhardness profiles was determined for each coating. Experimental procedures showed that mixture of powders is not effective procedure to achieve the modification of Stellite 6 coatings with neither graphite nor graphene. Results revealed that graphite modified coatings induced an increase in hardness whereas graphene modified coatings exhibit a behavior in hardness that depends on surface finishing. Dilution was increased with the addition of both powders revealing an interaction between powders, substrate and plasma arc.

Keywords: Plasma Transferred Arc, Graphite, Graphene, Stellite 6, Alloying

1. INTRODUCTION

Wear is one a degradation mechanism experience by engineering components that has the greatest impact on our society. This mechanism implies several losses, from financial losses, due to the loss of materials, energy and components, to human lives, when wear is the precursor of catastrophic accidents. A study developed by Holmberg and Erdemir (2017) estimates that approximately 23% of all energy consumed on the planet annually (approximately 119 EJ) is used in tribological contacts, with 20% needed to overcome friction and 3% for maintenance and new manufacturing of the damaged components. An approach adopted to mitigate wear phenomena is the use of hardfacing coatings.

The wear resistance depends on several factors, including material characteristics, as chemical composition, microstructure, Young modulus, processing technique and parameters, as well as the tribological system, that includes applied load, sliding distance, size and hardness of abrasive particles, as explained by Lin and Chen (2006).

One of the most used alloy systems for applications that require high wear resistance the Co-Cr-W-C. Within this system, Stellite 6 is most widely applied, its strength depending on two mechanisms: solid solution hardening and carbide distribution. The range of application is wide, reaching severe conditions. Jeshvaghani et al. (2011) report a high corrosion resistance, high hardness at high temperatures and high wear resistance under high pressure conditions.

Stellite 6 has a high coefficient of friction, resulting in a high loss of energy during its working cycle. The reduction of the coefficient of friction can be achieved using solid lubricants in the alloy, forming metallic matrix composites that have particles which act in the reduction of the coefficient of friction. Among the different materials used for such an application are graphite and graphene, that are allotropic forms of carbon, as demonstrated by Menezes et al. (2022).

According to Menezes et al. (2022), low coefficient of friction, high thermal stability, easy to shear crystalline structure, application temperature between 500 and 600 °C, are characteristics of graphite. Graphene, according to Ding et al. (2022), exhibits the following characteristics: high thermal and electrical conductivity, high surface area, good chemical inertness and high resistance to oxidation.

The tailoring of coatings modified by graphite and graphene has already been carried out by thermal spraying, friction welding and thin film techniques. Authors have not identified reports on hardfacing coatings processed by the plasma transferred arc process, modified with graphite and graphene as self-lubricating compounds and aim to contribute to a better understanding of the processing and characterization of Stellite based coating with a dispersion of graphene or graphite. In particular, it is aimed to evaluate the impact of the substrate surface finishing and pre-placed graphene and graphite particles layer in the transferred arc plasma processing of the Stellite 6 alloy.

2. EXPERIMENTAL PROCEDURE

An atomized commercially known as Stellite 6, a Co-Cr-W-C based alloy, with the chemical composition shown in Table 1 was used as reference material in this work and the substrate on which the coatings were applied is AISI 304L austenitic stainless steel plates (100×75×12,5mm). The graphite powder is the Micrograf HC30, kindly donated by the company Nacional de Grafite. The graphene nanoplatelets (specification 900412) were supplied by Sigma Aldrich. Data relating to the characteristics of all powders used, according to information provided by the manufacturers, are contained in Table 2.

Table 1. Weight composition of Stellite 6 powder and AISI 304L substrate.

Material	Weight composition, %								
	Co	Cr	W	C	Fe	Ni	Mo	Mn	Si
Stellite 6	Balance	28.00	4.50	1.20	< 3	< 2	< 1	< 2	< 3
AISI 304L	-	18.50	-	0.08	69.92	10.00	-	1.50	-

Table 2. General information of powders used in this work.

Item	Material	Manufacturer	Powder granulometry, μm			Density, kg/m^3	Apparent density, kg/m^3	ASE*, m^2/g
			D ₁₀	D ₅₀	D ₉₀			
1	Co-based alloy (Stellite 6)	Hoganas Belgium SA	50 - 200			8400	-	-
2	Graphene nanoplatelets	Sigma Aldrich	5			-	30-100	120-150
3	Graphite HC30	Nacional de Grafite	9.1	25.8	55.7	-	0.0098	25

*Surface specific area

Coatings were processed as single beads by Plasma Transferred Arc process (PTA) system. The processing parameters used in this work are shown in Table 3. It was used argon as a plasma, shielding and carrier gas.

Surface finishing of the substrate plates were produced in three different conditions, as shown in Table 4. After sanding, substrates were cleaned with anhydrous ethanol. To characterize the surface roughness of the substrate under the conditions used, the roughness measurement was carried out using three-dimensional profilometry with the confocal microscope.

Table 3. Processing parameters of PTA used in this work.

Description	Valor
Current, A	130
Plasma gas flow rate, l/min	2
Shielding gas flow rate, l/min	15
Carrier gas flow rate, l/min	1.5
Powder mass flow rate, g/min	10
Travel speed, mm/min	100
Stand-off distance, mm	10
Substrate temperature, °C	Room

Table 4. Substrate plate surface finishing.

Sample name	Description of substrate plate
S1	AISI 304L plate - as received
S2	AISI 304L plate - grinded with #36 sandpaper
S3	AISI 304L plate - grinded with #220 sandpaper

An initial approach tested the preparation of a powder mixtures of Stellite 6 and graphene or graphite to be fed through the feeder and inserted over the plasma arc. Plasma arc melts the powders and feeds them into the weld pool over the substrate. Another approached manually applied a film of graphite and graphene on the substrate, and subsequently, Stellite 6 alloy was PTA deposited on the substrate with the applied powder, Figure 1. The graphite and graphene powders pre-placed on the substrate were previously dispersed in anhydrous ethanol and stirred in an ultrasonic shaker for 90 minutes, before being applied. Subsequently, the substrates were placed in a furnace for evaporation of anhydrous ethanol and drying of the set, before processing, in order to remove moisture. The Stellite 6 powder was also stored in an stove for one day at a temperature of 50 °C, to remove eventual moisture before deposition.

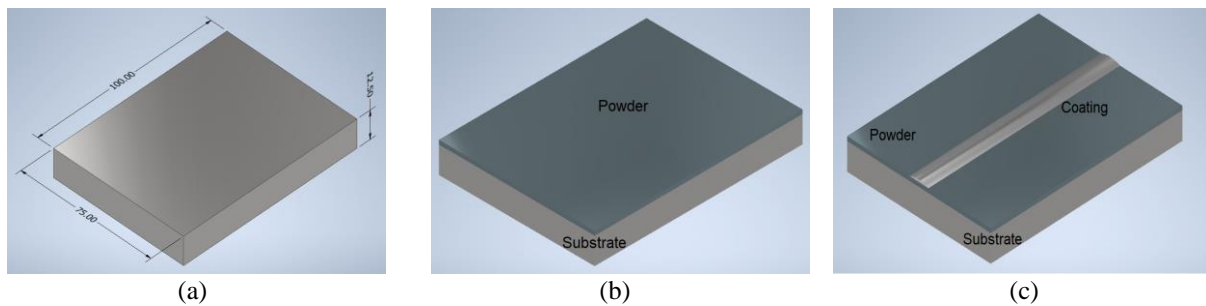


Figure 1. Coating development sequence. (a) Substrate, dimensions in mm, (b) powder applied over substrate and (c) coating applied over painted substrate.

Samples from coatings were removed and the cross section analyzed, using the metallographic cutter and grinding with silicon carbide papers with #180, #220, #300, #400, #600 and #1200 mesh and polishing with 1 micrometer alumina and colloidal silica.

The geometry of coatings was characterized for their surface appearance and cross section with help of stereo microscope. The width, reinforcement, penetration, wettability and dilution were measured, with help of ImageJ software, Figure 2. Dilution was also measured by the iron ratio in the center of the coating, determined by Energy-Dispersive X-ray Spectroscopy (EDS) and using Eq. (1). As mentioned by Gholipour et al. (2011), the EDS does not present satisfactory results for light elements and, therefore, we did not use the search for carbon in our samples.

Vickers microhardness profile of the processed coatings was carried out, mapping the microhardness along the coating, using a load of 100 grams for this test. A schematic representation of how the microhardness profiles were measured is shown in Figure 8 (d).

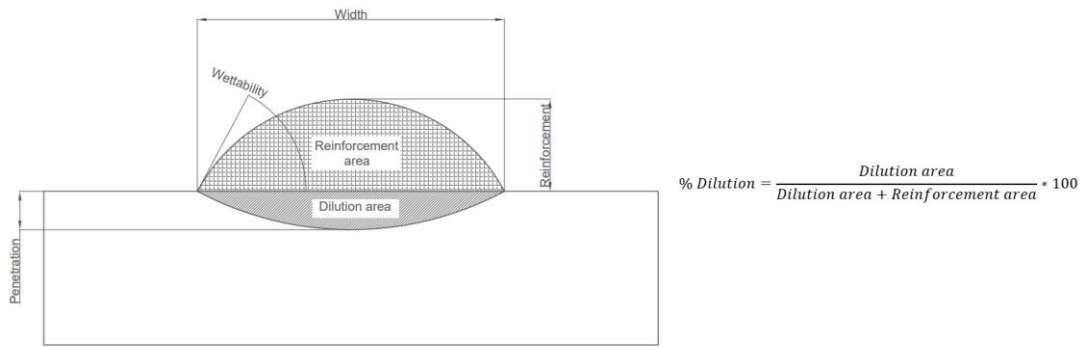


Figure 2. Coating characteristics and calculation of dilution by area method.

$$\% \text{ Dilution} = \frac{c_I - c_p}{c_s - c_p} \quad (1)$$

Where c_I – iron composition on layer of the substrate; c_p – iron composition of powder; c_s – iron composition of substrate.

The equipment list used in each step of characterization is shown in Table 5.

Table 5. Equipment list used in this work.

Test	Equipment model	Manufacturer
Stereo microscope	SZX10	Olympus
Scanning electron microscopy	Vega-3 LMU	Tescan
Energy-dispersive X-ray spectroscopy	Aztec Advanced	Oxford Instruments
Vickers microhardness	HMV-T2	Shimadzu
PTA Power Supply	Starweld 300 PTA Welding System	Stellite Inc
PTA Torch	Excalibur	Kennametal

3. RESULTS AND DISCUSSION

The first approach used to prepare and deposit powder mixture of Stellite 6 and graphene or graphite revealed a few challenges that compromised processing of coatings. The non-homogeneous mixture of powders (see Figure 3), showing large agglomerates of particles, had a low flowability. The mass flow rate was not constant, with clogging of the feed tube, which compromised the procedures to obtain coatings by the deposition of single tracks.

The alternative approached that used pre-placed powders before the deposition of Stellite 6 by PTA on substrates with different roughness offer better results.

The results of substrate profilometry are shown in Figure 4. The roughness obtained in each surface finishing is summarized in Table 6. The roughness of the as-received substrate is the highest, and several pits were identified on its surface. Comparing the sanded substrates, it is identified that the roughness of the smaller mesh sandpaper is greater.

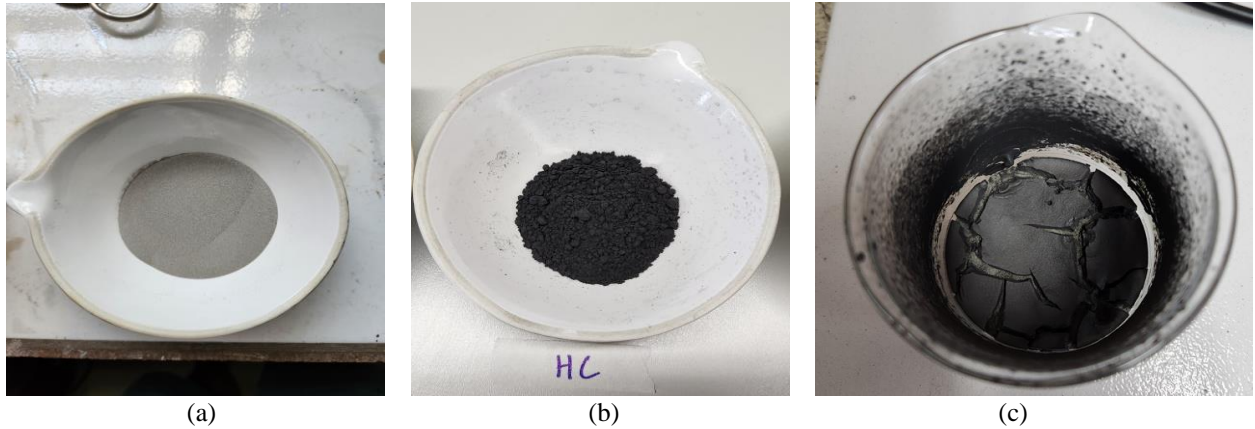


Figure 3. (a) Pure Stellite 6 powder, (b) pure graphite HC30 powder and (c) graphene-Stellite 6 mixed powder.

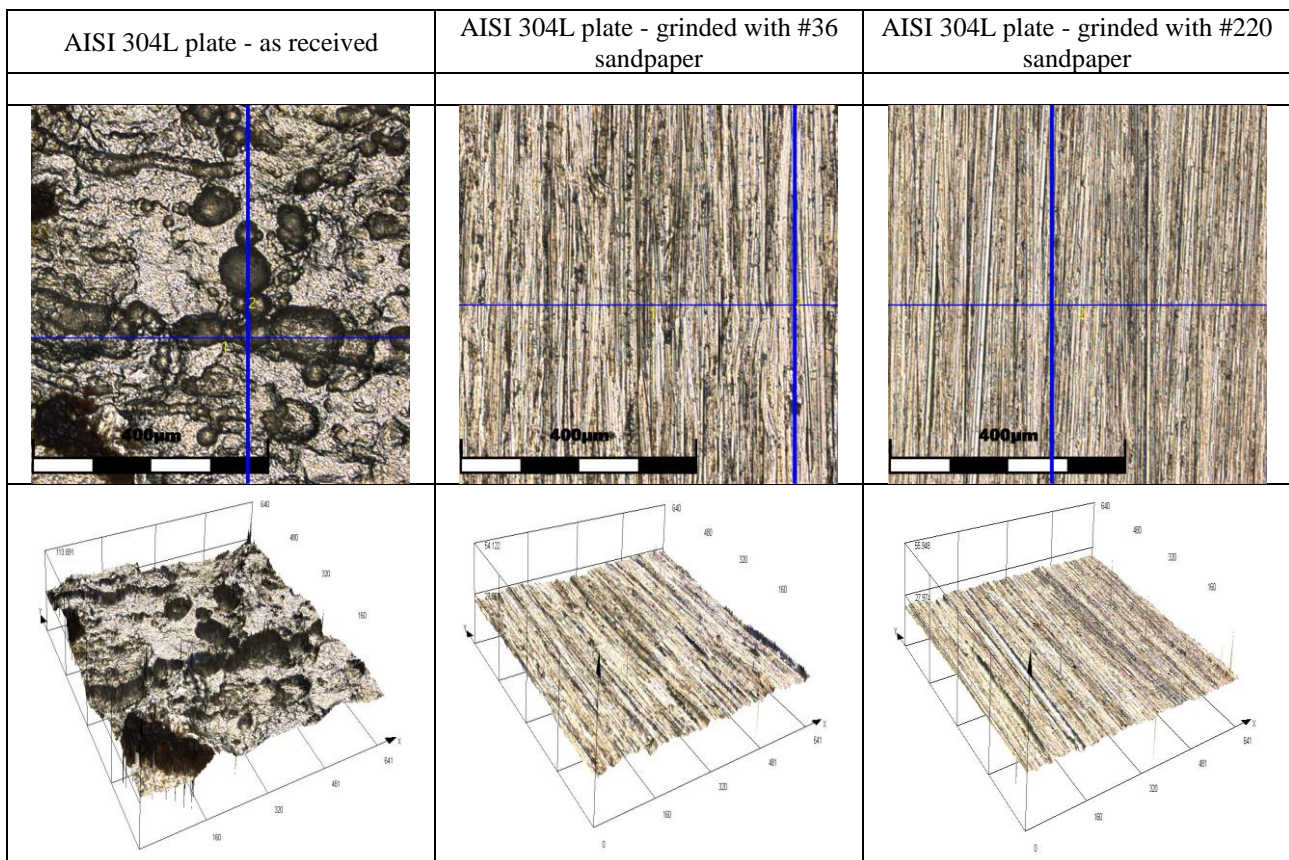


Figure 4. Surface aspect localization of measured linear roughness profile and 3D aspect of each substrate.

Table 6. Roughness of each substrate plate.

Substrate	Surface roughness, μm			
	Sq	Sp	Sv	Sz
As received	10.5	55.2	60.9	116.1
#36	1.4	28.8	25.4	54.1
#220	0.9	30.7	25.4	56.1

As shown in Figure 5, fluctuations in the linearity of graphene-modified coatings are identified. The other coatings presented a similar visual appearance, with no identifiable alterations in the visual inspection.

The cross section of the coatings, Figure 6, for substrates with different surface finish processed on the AISI 304L plate with and without the pre-placed graphene or graphite exhibit similar characteristics, except for the coating processed on graphene pre-placed film on a surface finished with a #36 mesh sandpaper, which showed great penetration.

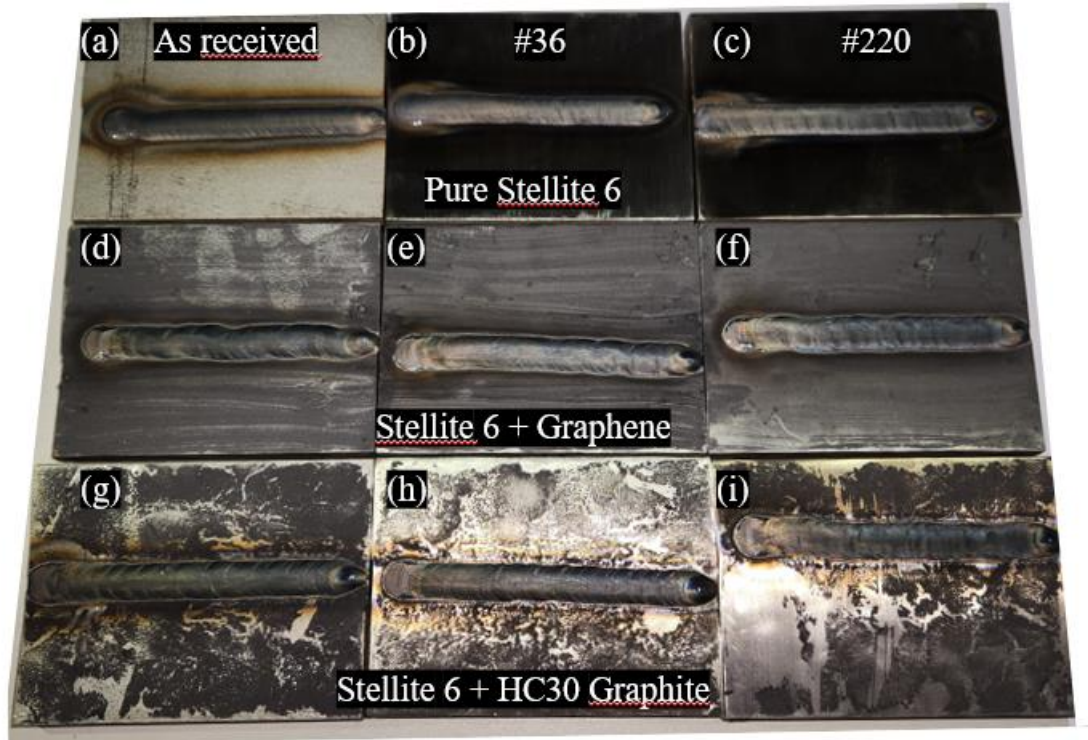


Figure 5. Coatings prepared by PTA for this work, immediately after the deposition, without any surface cleaning.

The measured geometric characteristics of each coating are presented in Figure 7. It is identified that the surface finishing impacted differently each chemical composition. Tested dilution increased for both surface finishes for the Stellite 6 alloy, but did not change with the graphite modification and showed a significant increase for the graphene-modified coating sanded with #36 mesh, which showed a high penetration. The other geometric characteristics of the coatings were similar.

An interesting point identified in this work is the great penetration of coatings processed on pre-placed graphene layer on substrates grinded with the #36 mesh sandpaper. The penetration is caused by greater melting of the substrate, inspite of the PTA processing being used with a fix set of parameters. Thus, it is concluded under this condition the graphene “trapped” in the roughness of the surface induces an interaction with the substrate, which ends up increasing the penetration of the coating. The causes for this behavior are still not completely understood and need further studies for their complete understanding. Some hypotheses for explaining this behavior, put forward by authors, are: greater anchorage of graphene particles in this roughness, the larger thermal conductivity of graphene account for a more significant heat transfer to the substrate; possible entrapment of higher quantity of graphene powder in the rough profile of the material, due to the interaction of its high surface area particles with the substrate, with subsequent oxidation of graphene, resulting in an exothermic reaction that increases the temperature at the fusion line. It is also possible that the electric arc exposure might have caused some of the graphene to turn into CO₂, modifying the plasma gas environment. This can cause the gas to have different ionization energies and heat conductivity capabilities, and the electric arc to have different sizes. Studies on the effect of welding gases show that the addition of CO₂ to inert Argon gas atmosphere can promote an increase in the depth of the weld and modify the shape of the weld bead to have a more well-spread penetration profile, rather than a narrower penetration profile.

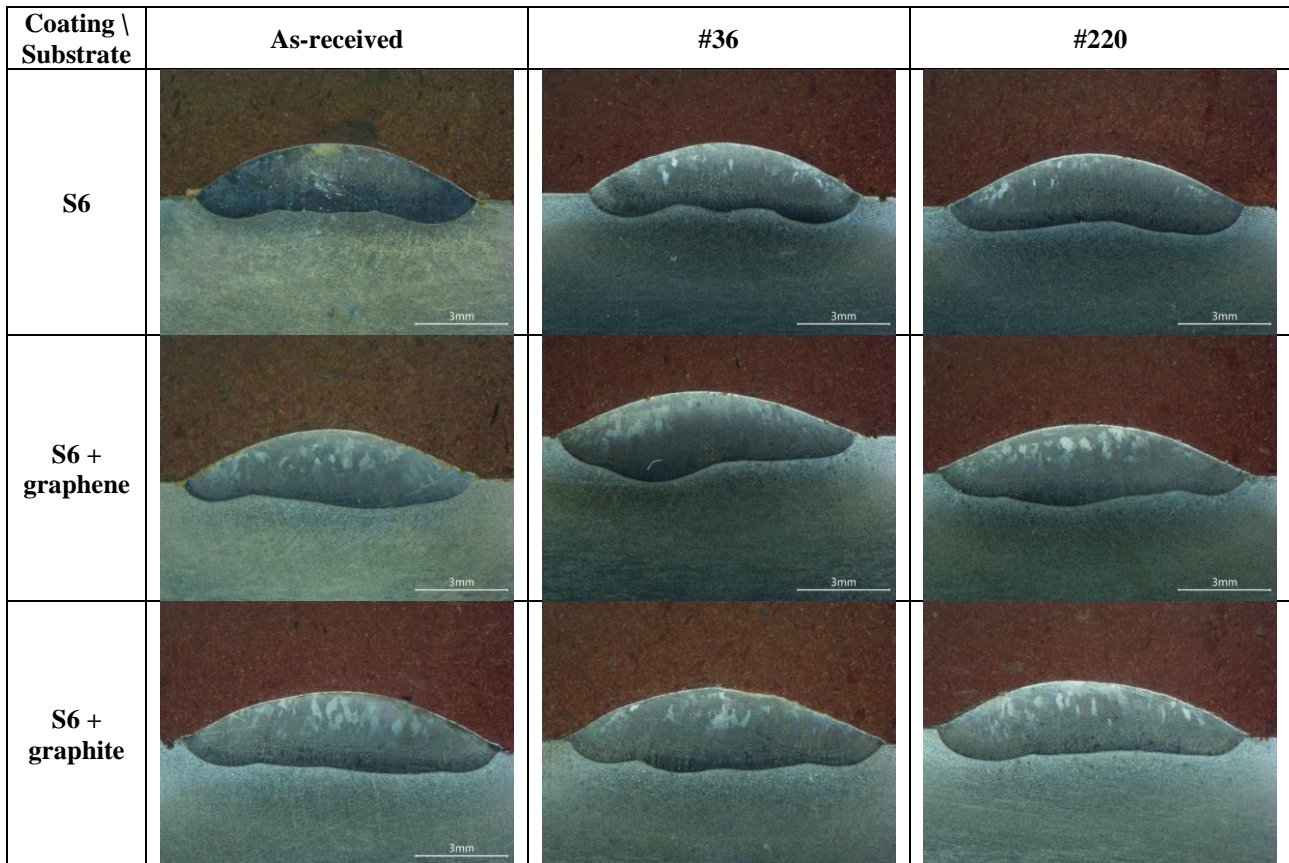
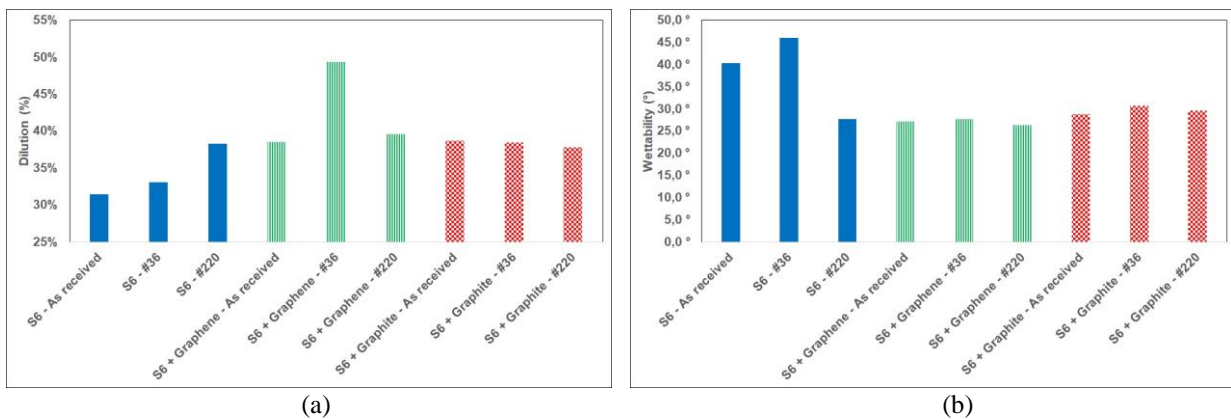


Figure 6. Cross section of each processed coating.

Vickers microhardness profiles of coatings are shown in Figure 8. Results confirmed the impact of different composition and surface finishing on the geometry of coatings as illustrated by the length of each profile. Due to the similarity of the results, the Tukey test was performed to identify whether the variations found are significant. The results of the measurements after applying the Tukey test are shown in Figure 9. Vickers microhardness of the graphite-modified samples did not show significant changes in relation to the surface finish of the substrate. Samples modified with graphene showed a different behavior, showing higher microhardness with the #220 sandpaper surface finishing and lower microhardness with the #36 sandpaper surface finishing, compared with as-received plate surface. The Stellite 6 alloy samples showed a reduction in microhardness with the surface finishing applied by both conditions.



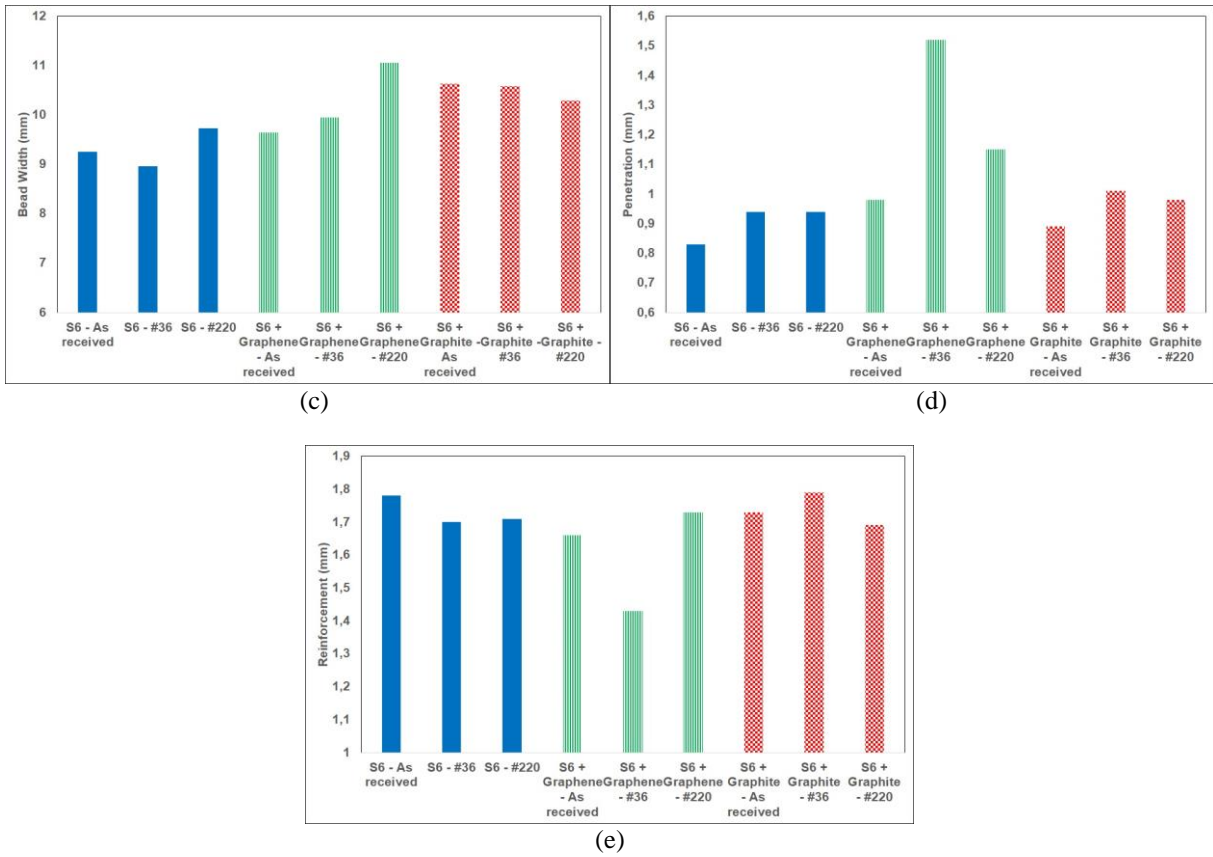


Figure 7. Geometric characteristics of coatings processed. (a) Dilution, (b) wettability (c) bead width, (d) penetration and (e) reinforcement.

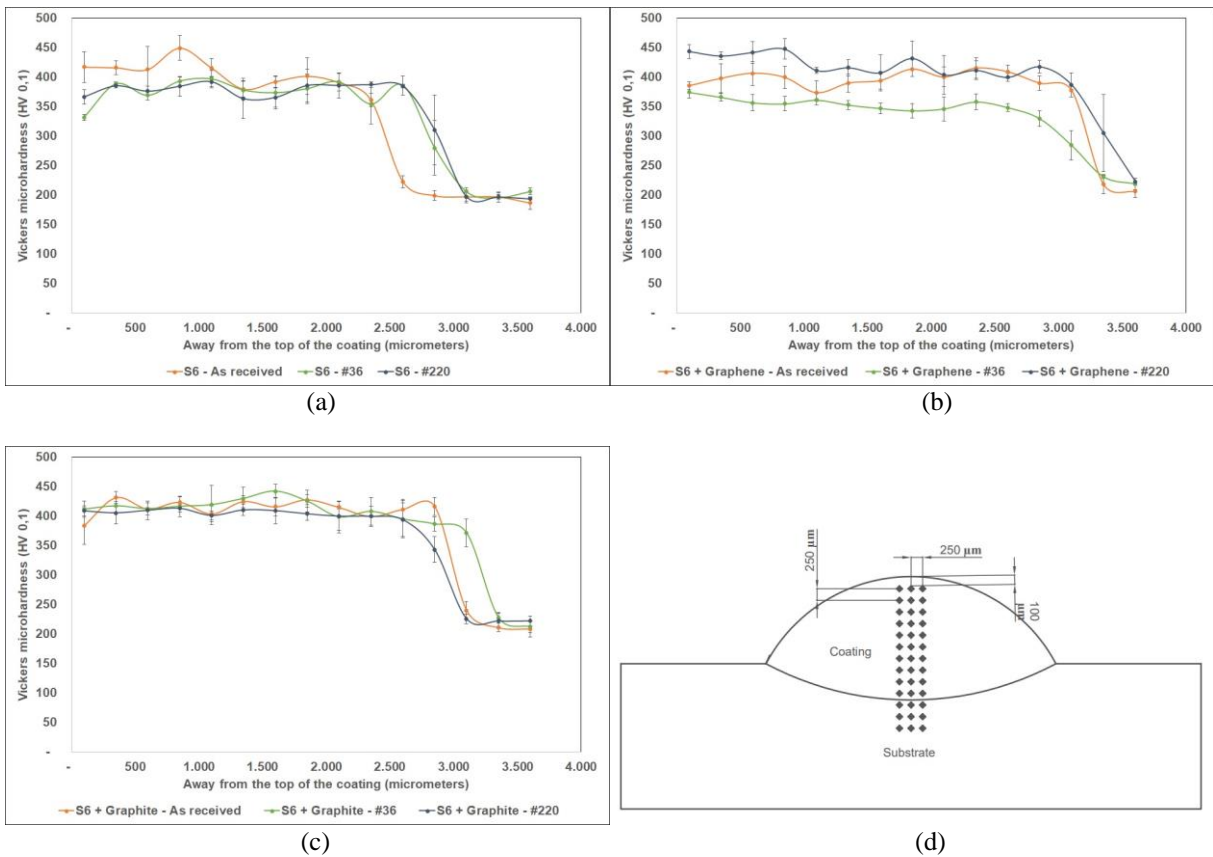


Figure 8. Vickers microhardness of each chemical composition in each substrate of (a) Stellite 6, (b) graphene pre-placed powder in substrate and (c) graphite pre-placed powder in substrate. (d) Schematic view of Vickers microhardness measurement, showing indentations on coating and substrate.

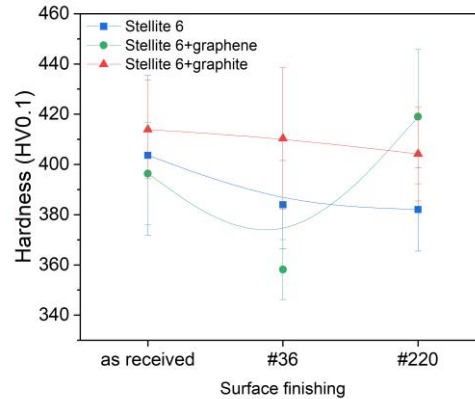


Figure 9. Vickers microhardness of each chemical composition after Tukey test.

The increasing the roughness of the substrate surface induced a reduction in the hardness of the Stellite 6 coatings. This behavior can be associated with an increase in dilution as the rougher the surface the easier is to melt the substrate surface. Similar trend was observed in coatings processed on the pre-placed layer of graphite although with an increase in the average coatings hardness, but the hardness reduction with increasing roughness of the substrate is not as pronounced. This behavior reveals that surface roughness did not play a role “trapping” the pre-placed graphite particles on the surface of the substrate before the deposition of the Co based alloy. However, depositing Stellite 6 on a graphene pre-placed layer induced changes in microhardness and dilution when compared to coatings deposited directly on the AISI 304 plate. The modification with graphene indicated that the surface roughness might have better “trapped” the nano particles of graphene on the surface as the its roughness is significant larger the graphene particles. This behavior apparently was more significant for the ratio roughness/particles size obtained after grinding with #220, accounting for the more significant increase in the average hardness of coatings.

Table 7. EDS results (%wt) for each coating and dilution measured by chemical composition on the center of coating.

Sample name	Chemical element weight, %					Dilution, %
	Co	Cr	W	Fe	Ni	
S6 - As received	41.7	25.6	3.9	24.9	3.9	32
S6 - #36	41.0	25.5	3.6	26.1	3.8	34
S6 + graphene - #36	31.4	24.8	3.1	35.6	5.0	48
S6 + graphite - #36	39.4	26.4	3.8	26.5	3.9	34

The processed Co-based alloy coatings exhibit Vickers microhardness lower than that informed by the manufacturer for this process (420 HV). This is a consequence of the processing parameters that determine heat input hence the interaction with the substrate but also of the procedure adopted to assess dilution. Yaedu and d’Oliveira show that dilution based on the Fe content has been reported to shown higher values than those measured based on the area ratio. The content of the iron in the center of the coating was measured by EDS and the results are shown in Table 7.

As the dilution affects the chemical composition of the coating, adding chemical elements from the substrate in the final solidification condition affects the strengthening mechanisms of the alloy. The reduction in microhardness can be attributed to the reduction of the solid solution strengthening mechanism in cobalt alloys. According to Gholipour et al. (2011), the chemical composition affects the properties of the alloy, with chromium, tungsten, tantalum, niobium and molybdenum improving its mechanical strength and iron increasing its toughness, but reducing corrosion resistance and hardness. In this study, the AISI 304L substrate mainly supplies iron for the coating when the dilution increases, a situation that is illustrated with the chemical compositions obtained with the EDS for the coatings in Table 7.

4. CONCLUSIONS

Under the conditions used in this investigation of the effect of graphene and graphite on the characteristics of a cobalt-based coating processed on AISI 304L plates with different surface roughness it is possible to conclude:

- It was possible to modify Stellite 6 single beads deposits with carbon-based materials using an indirect feeding strategy, where graphene and graphite particles were pre-placed onto the 304 stainless steel substrate (in the as received condition and after preparation using grinding with SiC paper with #36 and #220 mesh)
- Graphite additions were shown to increase the hardness of the coatings, for all surface finishing investigated, which could be associated to solid solution hardening, carbide formation or grain refinement (still under investigation);
- Roughness had a greater impact on the hardness of coating processed with graphene additions, where the highest hardness values were reached by the finest surface roughness, expected to account for the higher surface area, and possibly to a higher content of graphene;
- Graphene additions greatly affected the shape of the weld bead, accounting for a more well spread profile, with deep penetration and dilution. The effect of the entrapment of the graphene nanoparticles, the high thermal conductivity of graphene and/or a modification of the plasma gas atmosphere (by the formation of some CO₂) could be accounting for the observed behavior;
- The impact of a preplaced graphene layer on the processed coatings depends on the roughness of the substrate, with the higher hardness measured for coatings processed on a substrate roughness obtained with a #220 mesh sandpaper.

5. ACKNOWLEDGEMENTS

The authors would like to thank the following bodies/institutes listed below. This work could not have been carried out with your support: CNPQ, CAPES, Nacional de Grafite, SENAI, UFPR CME - Electronic Microscopy Center and CLabmu

6. REFERENCES

- Ding J. Zhao H., Yu H. 2022. Bioinspired strategies for making superior graphene composite coatings. *Chemical Engineering Journal*, Vol. 435.
- Gholipour A., Shamanian M., Ashrafizadeh F. 2011. Microstructure and wear behavior of stellite 6 cladding on 17-4 PH stainless steel. *Journal of Alloys and Compounds*, Vol. 509, pp. 4905–4909.
- Holmberg K., Erdemir A. 2017. Influence of tribology on global energy consumption costs and emissions. *Friction*, Vol. 5, pp. 263-284.
- Jeshvaghani R. A., Shamanian M., Jaberzadeh M. 2011. Enhancement of wear resistance of ductile iron surface alloyed by Stellite 6. *Materials & Design*, Vol. 32, pp. 2028-2033.
- Lin W. C., Chen C. 2006. Characteristics of thin surface layers of cobalt-based alloys deposited by laser cladding. *Surface and Coatings Technology*, Vol. 200, pp. 4557–4563.
- Menezes P. L., Rohatgi P. K., Omrani E. 2022. *Self-Lubricating Composites*. 2. ed. Springer.
- Yaedu A. E., d'Oliveira A. S. C. M. 2005. Cobalt based alloy PTA hardfacing on different substrate steels. *Materials Science and Technology*, Vol. 21, pp. 459-466.

7. RESPONSIBILITY NOTICE

The authors are the only responsible for the printed material included in this paper.